Neural network model for phase-height relationship of each image pixel in 3D shape measurement by machine vision

Byeong-mook Chung

School of Mechanical Engineering, Yeungnam University,
Gyeongsan 712-749, Korea; e-mail: bmchung@yu.ac.kr

In a three-dimensional measurement system based on a digital light processing projector and a camera, a height estimating function is very important. Sinusoidal fringe patterns of the projector are projected onto the object, and the phase of the measuring point is calculated from the camera image. Then, the height of the measuring point is inferred by the phase. The phase-to-height relationship is unique at each image point. However it is nonlinearly different according to the image coordinates. It is also difficult to obtain the geometrical model because of lens distortion. Even though some studies have been performed on neural network models to find the height from the phase and the related coordinates, the results are not good because of the complex relationship. Therefore, this paper proposes a hybrid method that combines a geometric analysis and a neural network model. The proposed method first finds the phase-to-height relationship from a geometric analysis for each image pixel, and then uses a neural network model to find the related parameters for the relationship. The experimental results show that the proposed method is superior to previous neural network methods.

Keywords: machine vision, shape measurement, fringe pattern projection, phase-height relationship, neural network.

1. Introduction

Three-dimensional (3D) measurement by using optical sensors has been extensively studied for applications because of the intrinsic noncontact nature of the measurement and its high speed [1]. A typical 3D measurement system based on a fringe pattern projection (FPP) system [2–6] is constructed by using a white light projector and a charge-coupled device (CCD) camera. The projector projects sinusoidal fringe patterns onto the object, and the CCD camera acquires the patterns that are deformed by the object's shape. The height information of the object is encoded into the deformed fringe pattern recorded by the CCD camera. In this measurement system, it is very important to obtain the phase-to-height relationship. There are various calibration methods to find the phase-to-height relationship [7]. The first method uses a simple look-up table (LUT) containing the relationship between phase values and heights for each

camera pixel [8]. The second method is based on measuring geometric parameters. This method relies on a certain measurement setup in which the geometric parameters and other parameters must be precisely determined in advance [9–11]. The third method is based on applying a least squares method to determine the phase-to-height relationship by using several standard gauge blocks [12–14]. Another possibility is the use of an artificial neural network (NN) to estimate the depth maps from the recovered phase distributions [15–18]. A NN has the advantages of high-speed parallel calculative activity, a powerful ability of function approximation, and resistance to noise.

Cuevas *et al*. used a radial basis function (RBF) based NN to calculate the height of an object from the demonstrated phase [15]. Because Cuevas *et al*. used the training planes with only three different heights (0, 30, 60 mm), the structure of the NN model is simple, but the modeling error is somewhat large. They proposed another multi-layer NN to obtain the relationship between the samples of the fringe pattern and the height directional gradients of the measured object [16]. Using this method, the height of the object can be recovered by integrating the height directional gradients measured by the network. However, it is very difficult to find the training sets because they used the fringe pattern irradiance instead of the phase value, and the modeling error is still as large as 0.8 mm. Ganotra *et al*. followed Cuevas and used a RBF NN and multi--layer NN to measure the height of the object [17]. The difference is the method to find the phase value. Because the methods cannot measure a free-form surface object, Yan *et al*. presented a method using a three-layer NN to measure the free-form surface object under the condition of fringe projection [18]. Their NN model was used to obtain only the phase value from the deformed fringe pattern. It was possible to measure a free-form surface object because they used the geometric parameter measuring method to obtain the height. Therefore, this paper suggests a new NN model based on a mathematical equation driven by a geometric analysis. This method uses a geometric equation for the phase-to-height relationship in each image pixel, and the related parameters are inferred by using the neural network model. In this case, the training set and the NN model are simple because the NN model uses two input variables for the image coordinates. Thus, better modeling results can be obtained.

2. Conventional multi-layer neural network for phase-to-height relationship

2.1. Geometric analysis

Figure 1 illustrates a typical setup of the generalized FPP system [12], wherein the reference plane Oxy, the camera imaging plane $O'x'y'$, and the projection plane $O''x''y''$ are arbitrarily arranged. In the figure, P represents an arbitrary point on the object; B indicates the imaging point of P; D indicates the original fringe point projected at P; and A and C denote the lens centers of the camera and the projector, respectively. For convenience and clarification, the coordinates of a point in a coordinate system are denoted by the corresponding coordinate symbols, and the symbol of the point is chosen as the subscript. For example, point P is denoted as (x_p, y_p, z_p), (x'_p, y'_p, z'_p),
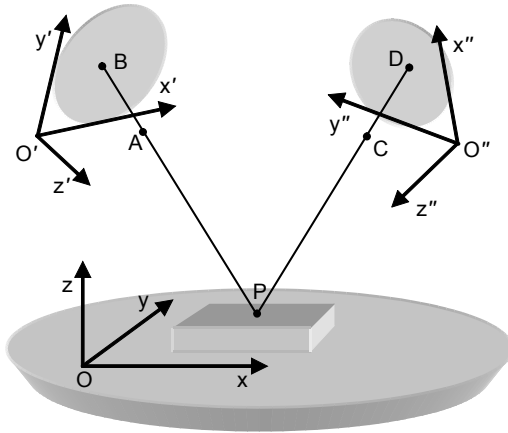
Fig. 1. Generalized FPP system based on the least squares method.

and (x''_p, y''_p, z''_p) in coordinate systems *Oxyz*, *O'x'y'z'*, and *O''x''y''z''*, respectively. Considering the coordinate relations among points *P*, *A*, and *B* in the system *Oxyz*, we obtain

$$\frac{x_P - x_A}{x_B - x_A} = \frac{y_P - y_A}{y_B - y_A} = \frac{z_P - z_A}{z_B - z_A} \tag{1}$$

A typical coordinate transformation of point *B* from system *O'x'y'z'* to system *Oxyz* can be described as follows:

$$\begin{bmatrix} x_B \\ y_B \\ z_B \end{bmatrix} = \begin{bmatrix} x_{O'} \\ y_{O'} \\ z_{O'} \end{bmatrix} + \mathrm{rot}(z, \gamma)\,\mathrm{rot}(y, \beta)\,\mathrm{rot}(x, \alpha) \begin{bmatrix} x'_B \\ y'_B \\ z'_B \end{bmatrix} \tag{2}$$

where $\mathrm{rot}(z, \gamma)$, $\mathrm{rot}(y, \beta)$ and $\mathrm{rot}(x, \alpha)$ are the coordinate transformation matrices, and α, β, and γ are the rotation angles of the *x'*, *y'*, and *z'* axes based on the reference coordinate system *Oxyz*, respectively. Finally, the height of the object based on the least squares method is as follows [12]:

$$z_p = \frac{c_0 + c_1\phi + (c_2 + c_3\phi)x'_B + (c_4 + c_5\phi)y'_B}{d_0 + d_1\phi + (d_2 + d_3\phi)x'_B + (d_4 + d_5\phi)y'_B} \tag{3}$$

where coefficients c_0 to c_5 and d_0 to d_5 are constants determined by geometric information such as the position and direction of the camera and the projector. The coefficients in the equation can be determined by using a nonlinear least squares algorithm such as the Levenberg–Marquardt method [12, 20], and a conventional linear algorithm can be used as well after the nonlinear least squares error is converted into a linear format. It is important to note that in addition to the reference plane of height zero,

using a single gauge object with a uniform height would produce indeterminate solutions for the nonlinear system of equations.

2.2. Multi-layer neural network

A multi-layer neural network (MLNN) is composed of several layers of inter-connected artificial neurons. Figure 2 shows the structure of a four layer neural network for the phase-to-height relationship. The first layer (the input layer) is used only to distribute three inputs for the u-v coordinates and the phase value to the neurons in the next layer. Hidden layers 1 and 2 are composed of R_1 and R_2 sigmoid neurons, respectively. The output layer has one sigmoid neuron and gives the height value as the output of the neural network. Each input is multiplied by a corresponding weight. The neuron's output is obtained by adding all weighted inputs and passing them through a non-linear activation function F. In general F is a sigmoid function. In many cases it is desirable to provide each neuron with a trainable bias. When the training process is executed, the weights are adjusted to minimize the squared error between the target output and the neural network output. To accomplish the training process, a training set S is necessary. The training set S is formed by training pair vectors. In the phase-to-height relationship described by Eq. (3), 3D points are used as the training vectors.
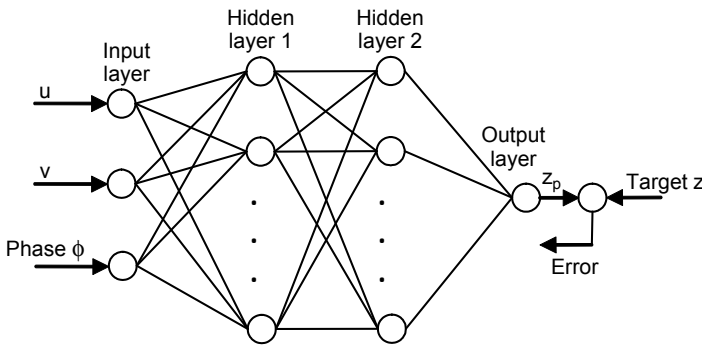

Fig. 2. Four-layer NN model for three inputs (u, v, ϕ) and one output (z_p).

CUEVAS *et al*. proposed a NN model with one hidden layer [15]. They used 75 radial-basis functions instead of sigmoid functions. Because they assumed that the phase--to-height relationship is linear within the given image coordinates, they trained for three different heights (0, 30, 60 mm). When they measured a small pyramid with an area of 90×90 mm and a height of 48 mm, the error of volume is 2.6% and the average error for height is 0.88 mm [16]. The error is too large to use the NN model in the 3D measurement system. In order to find the reason, we trained a NN model using three different heights (–25, 0, 25 mm). Then, Figure 3 shows the result that the error was as small as 0.2 mm for the trained heights but the error was as large as 2 mm for the other heights ($z = \pm 10$ mm). Therefore, to reduce the error, the training set needs to use more various heights for the train of NN model. If the measuring range is set to
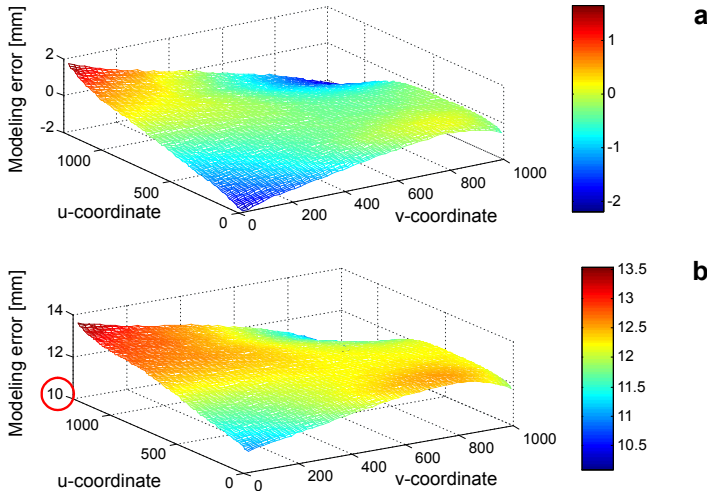
Fig. 3. Modeling result of plane $z = 0$ (**a**) and $z = 10$ mm (**b**) for the conventional NN model using 3 different heights.

$100 \times 100 \times 50$ mm for the x-y-z axis, the training point vectors must be able to represent the entire volume.

The view of the camera must be set in order to fully measure an area of 100×100 mm in the x-y plane. A height depth larger than 50 mm cannot be measured because the focal depth of the z-axis is relatively more sensitive than the x- and y-axes. To significantly reduce the error, we used 21 different heights (every 2.5 mm from -25 to $+25$ mm) for the z-axis and 127 different positions (every 10 pixels from 10 to 1270) for the u-axis. On the other hand, we used only nine different positions (every 100 pixels from 100 to 900) for the v-axis. The reason is as follows: if the fringe pattern of the projector is placed parallel to the v-axis of the camera, the phase value is almost the same with respect to the v-axis, except for the slight difference made by lens distortion. Therefore, the number of the training set S is 24 003 ($21 \times 127 \times 9$). Both the inputs and output of the network were pre- and post-processed to the range from -1 to $+1$ for better train-ing of the network. Using each target point, each weight was adjusted to minimize the error between the target height z and the neural network output z_p. However, it takes too much time to train the NN model if the training pair vectors are numerous.

It is very important to determine the number of hidden layers and the number of nodes in each hidden layer in order to find an optimal MLNN model. Table 1 shows the modeling results for various MLNNs according to the number of hidden layers. The average error is the average of the NN modeling errors for 5000 equally spaced points on the $z = 0$ plane. First, we used a NN model with one hidden layer. The average error after the training is reduced to 0.73, 0.46, and 0.43 mm when the number of nodes is increased to 100, 200, and 300, respectively. However, the error is reduced no more, even when the number of nodes is increased above 300. In this case, we need 1501 mem-

T a b l e 1. Average error according to hidden layers, nodes, and memory for conventional NN model (three inputs and one output).

Number of hidden layers	Number of node	Memory	Average error [mm]
1	100	501 ($3 \times 100 + 100 \times 1 + 101$)	0.73
	200	1001 ($3 \times 200 + 200 \times 1 + 201$)	0.46
	300	**1501 ($3 \times 300 + 300 \times 1 + 301$)**	**0.43**
2	5 + 5 = 10	56 ($3 \times 5 + 5 \times 5 + 5 \times 1 + 11$)	0.45
	10 + 10 = 20	**161 ($3 \times 10 + 10 \times 10 + 10 + 21$)**	**0.33**

ories because the number of weighting factors between two nodes is 1200 and the number of neuron biases in each node is 301. Next, we used a NN model with two hidden layers. The average error after the training is reduced to 0.45 mm when the number of nodes in the first hidden layer and the second hidden layer is 5 and 5, respectively. The average error is reduced to 0.33 mm when the number of nodes is 10 + 10. For 10 + 10 hidden layers, we only used 161 memories for 140 weighting factors and 21 neuron biases. However, the error is not reduced further, even when the number of nodes is increased above 20 (10 + 10). For three hidden layers, we cannot obtain any NN model because the modeling error is not reduced using the back-propagation algorithm. In conclusion, the optimal NN model is the four-layer NN model with two hidden layers and 10 + 10 nodes. Figure 4 shows the modeling errors of the four-layer NN model of which the average error is 0.33 mm. The error of the $z = 10$ plane is similar to that of the $z = 0$ plane because the height of $z = 10$ is included in the training set. Although the errors are small in the center area, they are as large as ±1 mm elsewhere. The model-
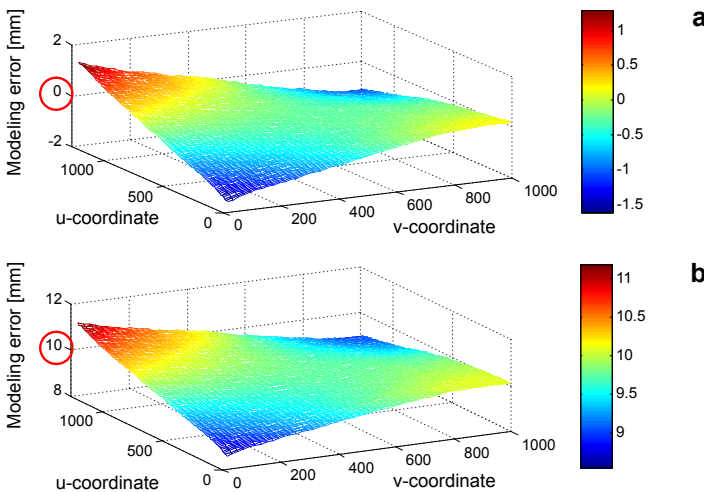

Fig. 4. Modeling result of plane $z = 0$ (**a**) and $z = 10$ mm (**b**) for the conventional NN model using 21 different heights.

ing results are better than Cuevas' results because the NN model used more height training vectors and more hidden-layers.

3. Proposed neural network for phase-to-height relationship

Equation (3) is the most general expression for the phase-to-height relationship. The equation has three inputs such as the image coordinates (x'_B, y'_B) and the phase value ϕ. However, a NN model with three inputs needs a 3D complex training set, and this makes it difficult to train the NN model. Therefore, we propose a simplified NN model that reduces the number of the inputs in the phase-to-height relationship. If the image coordinates are constant in Eq. (3), the equation is simplified by

$$z_p = \frac{c'_0 + c'_1\phi}{d'_0 + d'_1\phi} = h' + \frac{b'}{a' + \phi} \tag{4}$$

where $h' = c'_1/d'_1$, $a' = d'_0/d'_1$, and $b' = (c'_0 - c'_1 d'_0/d'_1)/d'_1$. Consider the physical meaning of h', a', and b'. If the fringe patterns set to be parallel to the *v*-axis of the image plane, Fig. 1 can be expressed in the *x-z* plane because the phase value is constant for the *v*-axis. Figure 5 shows the *x-z* plane including the image coordinates $(u = x'_B)$ for any *v*-coordinate $(v = y'_B)$ in the measurement system of Fig. 1. The points *C* and *P* are the optical center of the image lens and the optical center of the projection lens, respectively. The height of the object is obtained by finding the intersection point of the projection line and image line. If *H* is the height of the light source from the ref-
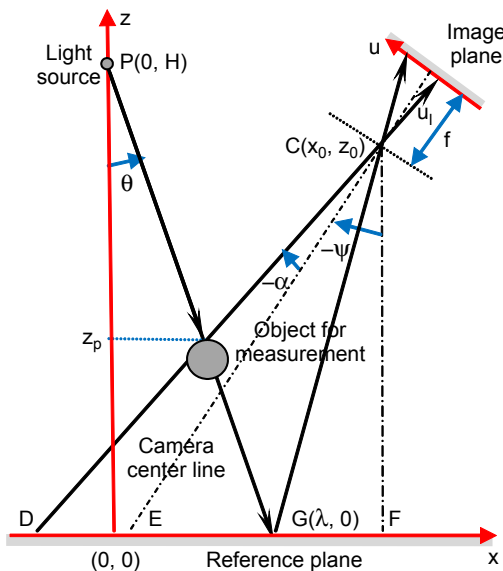

Fig. 5. Plane analysis for phase-to-height relationship.

erence plane, the equation of projection line PG with angle θ about the z-axis can be easily obtained. The equation of image line CD can also be obtained when the coordinate of the camera focus is (x_0, z_0) and the angle of the image line about the z-axis is $(\alpha + \psi)$. The height of an intersection point of two lines PG and CD can be obtained by [19]

$$z_p = H + \frac{x_0 - (H - z_0)\tan(\alpha + \psi)}{\tan(\alpha + \psi) - \tan(\theta)} \tag{5}$$

Then, the relationship between the real phase θ and the fringe phase ϕ is as follows:

$$\tan(\theta) = \frac{\lambda}{H} \cong \frac{k(\phi - \phi_0)}{H} = \eta(\phi - \phi_0) \tag{6}$$

where k, η and ϕ_0 are constant. When the height of the object is measured from the specific image coordinates (x_B', y_B'), it is determined only by θ because $\tan(\alpha + \psi)$ is constant. Then, in order to compare Eq. (5) with Eq. (4), it can be rewritten as

$$z_p = H - \frac{(H - z_0)\tan(\alpha + \psi) - x_0}{\tan(\alpha + \psi) - \eta(\phi - \phi_0)} = H - \frac{b}{a - \phi} \tag{7}$$

where

$$H = h' \tag{8}$$

$$a = -a' = \frac{\tan(\alpha + \psi)}{\eta} + \phi_0 \tag{9}$$

$$b = b' = \frac{(H - z_0)\tan(\alpha + \psi)}{\eta} - \frac{x_0}{\eta} \tag{10}$$

Therefore, h' is the height of the light source from the reference plane, and a' and b' are variables determined by the image coordinates (x_B', y_B'). If the fringe phase measured from an image coordinates is known, the height of the object can be obtained. Because the height is the z-coordinate, the x- and y-coordinates can be calculated by using a coordinate transformation equation such as Eq. (2). The variables a and b in Eq. (7) can be obtained if the corresponding phase values are measured for the given heights in each image pixel. The values a and b are obtained by using a least squares method for three more different heights. Figure 6 shows the proposed NN model. The input of the NN model is comprised of x- and y-coordinates of the image pixel, and the output is the coefficients of Eq. (7). When a phase value in a specific image pixel is measured, the height can be estimated because the NN model gives the coefficients. The proposed NN model used only 1143 (127 × 9) training members because the model needs a 2D training set. Fewer training members result in a faster training
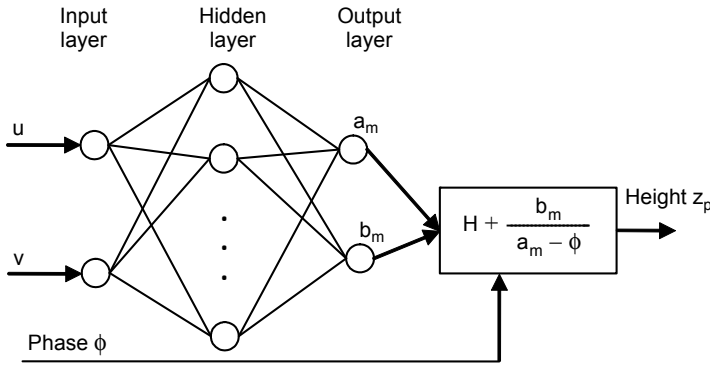
Fig. 6. Neural network model for two inputs (u, v) and two outputs (a_m, b_m).

time. Therefore, the training speed is about 20 times faster than that of the case using a 3D training set.

Table 2 shows the modeling results for various MLNN according to the number of hidden layers for the proposed model. Similar to previous experiments, the average error is the average of NN modeling errors for 5000 equally spaced points on the $z = 0$ plane. First, a NN model for one hidden layer was trained. When the number of nodes from 20 to 100 was increased, the average error after the training was reduced from 0.11 to 0.05 mm. Although the number of nodes was increased above 100, the error was not reduced. In this case, 502 memories are needed because the number of weighting factors is 400 and the number of neuron biases is 102. Next, a NN model with two hidden layers was trained. When the number of nodes from 10 (5 + 5) to 40 (20 + 20) was increased, the average error after the training was reduced from 0.28 to 0.05 mm. The error was not reduced further even when the number of nodes was increased above 40 522 memories are needed for 480 weighting factors and 42 neuron biases. In conclusion, it is possible to reduce the average error to 0.05 mm if the memory of the training weights is increased regardless of the number of hidden layers in the pro-

T a b l e 2. Average error according to hidden layers, nodes, and memory for the proposed NN model (two inputs and two outputs).

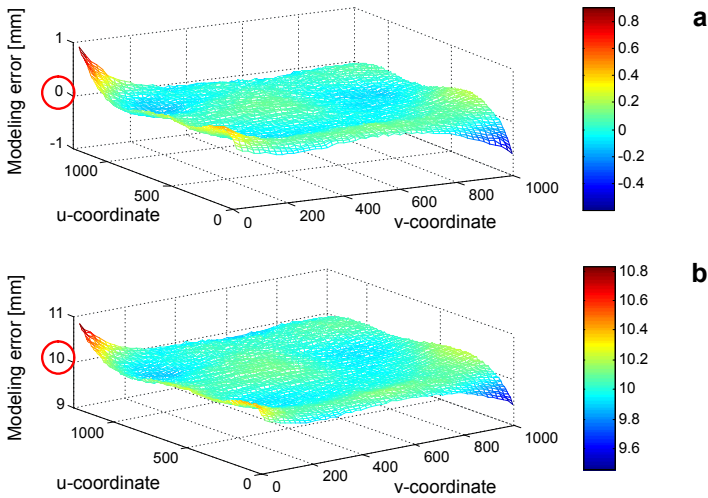| Number of hidden layers	Number of node	Memory	Average error [mm]
1	20	102 (2 × 20 + 20 × 2 + 22)	0.11
	50	252 (2 × 50 + 50 × 2 + 52)	0.08
	100	**502 (2 × 100 + 100 × 2 + 102)**	**0.05**
2	5 + 5 = 10	57 (2 × 5 + 5 × 5 + 5 × 2 + 12)	0.28
	10 + 10 = 20	162 (140 + 22)	0.13
	15 + 15 = 30	317 (285 + 32)	0.07
	20 + 20 = 40	**522 (480 + 42)**	**0.05**

Fig. 7. Modeling result of plane $z = 0$ (**a**) and $z = 10$ mm (**b**) using the proposed NN model.

posed NN model. Figure 7 shows modeling errors for the $z = 0$ and $z = 10$ planes, and the average error is 0.05 mm when the three-layer NN model used one hidden layer with 100 nodes. The results show that the errors are very small at the border area as well as in the center area.

4. Experiments

Figure 8 shows 3D measurement equipment using cameras and a beam projector. The equipment consists of black and white CCD cameras (AOS MPX1350, 1280×1024 pixels, and 8-bit data depth), a digital light processing (DLP) projector (LG HS200G, 800×600 pixels), a personal computer for image processing, and a three--axis stage for camera calibration. The stage has a repeatability accuracy of 0.001 mm, and the z-axis is only used to obtain focuses of the projector and camera during
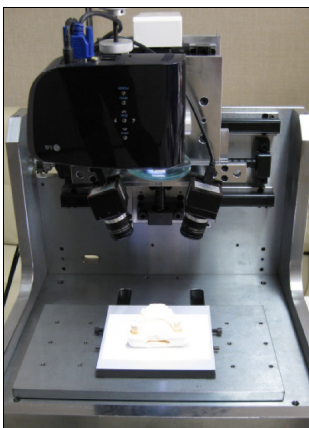

Fig. 8. 3D measurement equipment using the camera and projection Moirè.

the calibration for 3D measurement. In the experiments, the basic period of the fringe pattern was set to eight pixels, and the eight-bucket algorithm with eight different phases was used in the phase shift method. Because the horizontal resolution of the projector is 800 pixels, the gray code patterns of seven bits were necessary to distinguish 100 different periods. The measuring range was set to $100 \times 100 \times 50$ mm for the x-y-z axis because the focal depth of the z-axis is relatively sensitive to the x- and y-axes.

The $h-\theta$ relationships for 21 different heights (every 2.5 mm from –25 to +25 mm) are used to find the three unknown constants (a, b, H) in Eq. (9). From the calibration, H was found to be 275 mm regardless of the image coordinates. This means that the focus of the projector lens was 275 mm from the reference plane. The variables a and b must be found for every image pixel. Figure 9 shows the experimental results for the coefficients a and b for the horizontal line of $v = 500$ in the image plane of the camera with 1280×1024 pixels. As the position of image pixel u increases, the value of a also decreas from 500 to –200, whereas the value of b decreases from 160000 to 90000. Thus, the graph for b is plotted as $b/100$ to adjust the scale, as shown in Fig. 9.
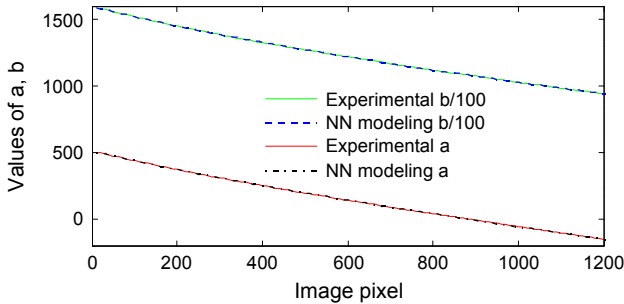

Fig. 9. Comparison between experimental values and NN model for a and b.

When the experimental values of a and b are obtained for each pixel, two million memories for 1280×1024 pixels are necessary. However, only 500 memories are enough if we train a 2×2 NN model as shown in Table 2. All of the network weights and neuron biases must be set to initial values before training starts. It is common practice with a NN to randomize the weights to small numbers. All inputs, outputs, weights, and biases are normalized. We used 1143 (127×9) 2D vectors as a training set because the 2×2 NN model has two inputs. It took 25 min for the training of 100000 iterations. As shown in Fig. 9, the blue dashed line represents modeling results for coefficient b, and the black chain line represents modeling results for coefficient a. We know that the two modeling lines are nearly equal to the experimental lines, respectively. Next, the other heights are measured using the modeling coefficients a and b in Eq. (9). Although Fig. 7 shows the modeling errors for the $z = 0$ and $z = 10$ planes, the errors are very large at the extreme border area. However, the border area is excluded in the measurement system because of lens distortion. The error is greatly reduced if 90% of the total image area is considered except the extreme border area. Figure 10 shows the modeling errors for the $z = 20$ and $z = -20$ planes when the image area is 1180×900.
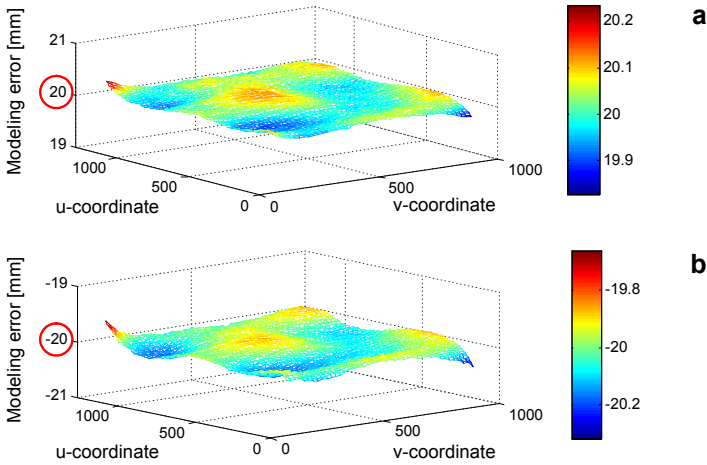
Fig. 10. Modeling result of plane $z = 20$ mm (**a**) and $z = -20$ mm (**b**) using the proposed 2×2 NN model.

The error shapes are similar to those of Fig. 7 except the extreme border area. The modeling errors in both planes are smaller than 0.01 mm.

5. Conclusions

A conventional NN model for the phase-to-height relationship has three inputs and one output in 3D shape measurement. The model needs a 3D training set to train the overall measuring volume. It is very difficult to train the NN model if the training members are too many. Therefore, this paper proposes a two-stage analysis method to obtain the phase-to-height relationship. After obtaining the phase-to-height relationship in each image pixel, the corresponding coefficients of the relationship are trained by the proposed NN model. The proposed NN model has two inputs and two outputs instead of three inputs and one output. The merit of a NN model with two inputs is that it is possible to use a 2D training set. The training time is faster and the accuracy is improved when 2D training members are used. Above all, the modeling error is significantly reduced from 0.33 to 0.05 mm. In conclusion, until now, it has been difficult to use the conventional NN model because of large modeling errors. Because the proposed NN model is based on accurate phase-to-height relationships and a short training time, it is possible to measure the accurate height of an object in 3D measurement.

References

[1] Chen F., Brown G.M., Song M., *Overview of three-dimensional shape measurement using optical methods*, Optical Engineering **39**(1), 2000, pp. 10–22.
[2] Yingsong Hu, Jiangtao Xi, Enbang Li, Joe Chicharo, Zongkai Yang, *Three-dimensional profilometry based on shift estimation of projected fringe patterns*, Applied Optics **45**(4), 2006, pp. 678–687.

[3] WEI-HUNG SU, KEBIN SHI, ZHIWEN LIU, BO WANG, REICHARD K., SHIZHUO YIN, A *large-depth-of-field projected fringe profilometry using supercontinuum light illumination*, Optics Express **13**(3), 2005, pp. 1025–1032.

[4] SANSONI G., CAROCCI M., RODELLA R., *Three-dimensional vision based on a combination of gray--code and phase-shift light projection: analysis and compensation of the systematic errors*, Applied Optics **38**(31), 1999, pp. 6565–6573.

[5] FEIPENG DA, SHAOYAN GAI, *Flexible three-dimensional measurement technique based on a digital light processing projector*, Applied Optics **47**(3), 2008, pp. 377–385.

[6] YI-BAE CHOI, SEUNG-WOO KIM, *Phase-shifting grating projection Moire topography*, Optical Engineering **37**(3), 1998, pp. 1005–1010.

[7] LEI HUANG, CHUA P.S.K., ASUNDI A., *Least-squares calibration method for fringe projection profilometry considering camera lens distortion*, Applied Optics **49**(9), 2010, pp. 1539–1548.

[8] HONGYU LIU, WEI-HUNG SU, REICHARD K., SHIZHUO YIN, *Calibration-based phase-shifting projected fringe profilometry for accurate absolute 3D surface profile measurement*, Optics Communications **216**(1–3), 2003, pp. 65–80.

[9] TAKEDA M., MUTOH K., *Fourier transform profilometry for the automatic measurement of 3D object shapes*, Applied Optics **22**(24), 1983, pp. 3977–3982.

[10] QINGYING HU, PEISEN S. HUANG, QIONGLIN FU, FU-PEN CHIANG, *Calibration of a three-dimensional shape measurement system*, Optical Engineering **42**(2), 2003, pp. 487–493.

[11] MAURE A., COBELLI P., PAGNEUX V., PETITJEANS P., *Experimental and theoretical inspection of the phase-to-height relation in Fourier transform profilometry*, Applied Optics **48**(2), 2009, pp. 380–392.

[12] HUA DU, ZHAOYANG WANG, *Three-dimensional shape measurement with an arbitrarily arranged fringe projection profilometry system*, Optics Letters **32**(16), 2007, pp. 2438–2440.

[13] HONGWEI GUO, HAITAO HE, YINGJIE YU, MINGYI CHEN, *Least-squares calibration method for fringe projection profilometry*, Optical Engineering **44**(3), 2005, article 033603.

[14] WENGUO LI, SUPING FANG, SHAOJUN DUAN, *3D shape measurement based on structured light projection applying polynomial interpolation technique*, Optik – International Journal for Light and Electron Optics **124**(1), 2013, pp. 20–27.

[15] CUEVAS F., SERVIN M., RODRIGUEZ-VERA R., *Depth object recovery using radial basis functions*, Optics Communications **163**(4–6), 1999, pp. 270–277.

[16] CUEVAS F., SERVIN M., STAVROUDIS O., RODRIGUEZ-VERA R., *Multi-layer neural network applied to phase and depth recovery from fringe patterns*, Optics Communications **181**(4–6), 2000, pp. 239–259.

[17] DINESH GANOTRA, JOBY JOSEPH, KEHAR SINGH, *Profilometry for the measurement of three-dimensional object shape using radial basis function, and multi-layer perceptron neural networks*, Optics Communications **209**(4–6), 2002, pp. 291–301.

[18] YAN TANGY, WEN-JING CHEN, XIAN-YU SU, LI-QUN XIANG, *Neural network applied to reconstruction of complex objects based on fringe projection*, Optics Communications **278**(2), 2007, pp. 274–278.

[19] BYEONG-MOOK CHUNG, YOON-CHANG PARK, *Hybrid method for phase-to-height relationship in 3D shape measurement using fringe pattern projection*, International Journal of Precision Engineering and Manufacturing **15**(3), 2014, pp. 407–413.

[20] MARQUARDT D., *An algorithm for least-squares estimation of nonlinear parameters*, Journal of the Society for Industrial and Applied Mathematics **11**, 1963, pp. 431–441.